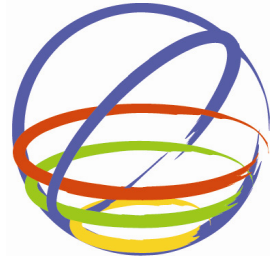


Development of MPS method for Earthquake Response Analysis Considering Collapse



15 WCEE
LISBOA 2012

I.Yoshida

Tokyo City University, Japan

SUMMARY:

Conventional FEM has a difficulty to simulate strong nonlinear behavior such as failure or collapse. DEM is one of the most successful methods to simulate the slope collapse. Its drawback is, however, that it is an empirical method, in which values of spring and dashpot to connect each particle must be determined empirically. In addition, theoretically DEM does not satisfy the wave equation exactly. MPS method is derived mathematically from a wave equation. Its formulation is very close to that of DEM. Consequently MPS method has capability similar to DEM with respect to failure phenomenon. The formulation of MPS method is illustrated for earthquake response simulation of slope. Viscous boundary and particle wise Rayleigh damping for MPS method are proposed and verified through comparison with simulation result by two dimensional FEM. Numerical simulation of slope collapse experiment is also demonstrated by MPS method.

Keywords: particle method, MPS, collapse of slope, earthquake response

1. INTRODUCTION

Needs for evaluation of ultimate limit state are increasing in Japan, partially because design earthquake motion is revised through the experience of large earthquakes occurred recently. Deformation is sometimes used to define ultimate limit state for geotechnical structures like a slope. There are several prospective methods to estimate large deformation, such as SPH (Smoothed Particle Hydrodynamics), MPS (Moving Particle Simulation), DEM (Discrete Element Method), MPM (Material Point Method), which are still in the stage of research. DEM is one of the most successful methods to simulate the failure or collapse of slope, but its drawback is that it is an empirical method, in which values of spring and dashpot to connect each particle must be determined empirically. In addition, theoretically DEM does not satisfy the wave equation. MPS method has advantage compared with DEM because it is derived mathematically from the wave equation. Its formulation is, however, very close to that of DEM, consequently MPS method has capability similar to DEM with respect to failure phenomenon. MPS method can be interpreted as extended DEM that satisfies the wave equation. It was originally developed for fluid analysis (Koshizuka et al. 1995, Koshizuka et al. 1996). The idea of the method was applied to elastic body (Chikazawa et al. 2001). MPS stands for Moving Particle Semi-implicit originally because semi-implicit scheme is used to solve the equation in fluid analysis. An explicit scheme is, however, used in elastic body analysis. The term, Moving Particle Simulation is sometimes used when the method for elastic body is referred.

The formulation of MPS method is illustrated for earthquake response simulation of slope. Viscous boundary and element-wise Rayleigh damping are important functions in earthquake response analysis and are often used in FEM (Finite Element Method). Viscous boundary and particle wise Rayleigh damping for MPS method are proposed and verified through comparison with simulation result by two dimensional FEM. Numerical simulation of slope collapse experiment is also demonstrated by MPS method.

2. FORMULATION OF MPS METHOD

2.1. Wave Propagation

2.1.1. Strain and stress in MPS Method

Initial and current vector from i to j $\mathbf{r}_{ij}^0, \mathbf{r}_{ij}$ are defined by using initial position vector \mathbf{r}^0 and current position vector \mathbf{r} .

$$\mathbf{r}_{ij}^0 = \mathbf{r}_j^0 - \mathbf{r}_i^0, \quad \mathbf{r}_{ij} = \mathbf{r}_j - \mathbf{r}_i \quad (1)$$

MPS method has a degree of freedom with respect to rotation of particle i , θ_i . Deformation vector \mathbf{u}_{ij} is obtained by removing the rigid rotation.

$$\mathbf{u}_{ij} = \mathbf{r}_{ij} - \mathbf{R}\mathbf{r}_{ij}^0, \quad \text{where, } \mathbf{R} = \begin{bmatrix} \cos \theta_{ij} & -\sin \theta_{ij} \\ \sin \theta_{ij} & \cos \theta_{ij} \end{bmatrix}, \quad \theta_{ij} = \frac{\theta_i + \theta_j}{2} \quad (2)$$

The current deformation vector \mathbf{u}_{ij} is decomposed into normal direction \mathbf{u}_{ij}^n (direction of \mathbf{r}_{ij}) and shear direction \mathbf{u}_{ij}^s (perpendicular to normal direction).

$$\mathbf{u}_{ij}^n = \frac{\mathbf{u}_{ij} \cdot \mathbf{r}_{ij}}{\|\mathbf{r}_{ij}\|} \frac{\mathbf{r}_{ij}}{\|\mathbf{r}_{ij}\|} \quad (3) \quad \mathbf{u}_{ij}^s = \mathbf{u}_{ij} - \mathbf{u}_{ij}^n \quad (4)$$

Normal stress σ_{ij}^n related to Lame's constant μ is formulated with normal strain ϵ_{ij}^n .

$$\sigma_{ij}^n = 2 \frac{(\mu_i + \mu_j)}{2} \epsilon_{ij}^n = (\mu_i + \mu_j) \frac{\mathbf{u}_{ij}^n}{\|\mathbf{r}_{ij}^0\|} = (\mu_i + \mu_j) \frac{c_{ij}^n}{\|\mathbf{r}_{ij}^0\|} \mathbf{r}_{ij}, \quad \text{where } c_{ij}^n = \frac{\mathbf{u}_{ij} \cdot \mathbf{r}_{ij}}{\|\mathbf{r}_{ij}\|} \quad (5)$$

Similarly, shear stress related to Lame's constant μ is formulated with shear strain.

$$\sigma_{ij}^s = 2 \frac{(\mu_i + \mu_j)}{2} \epsilon_{ij}^s = (\mu_i + \mu_j) \frac{\mathbf{u}_{ij}^s}{\|\mathbf{r}_{ij}^0\|} = (\mu_i + \mu_j) \frac{\mathbf{u}_{ij} - \mathbf{u}_{ij}^n}{\|\mathbf{r}_{ij}^0\|} \quad (6)$$

2.1.2. Equilibrium of force

The force acting on a particle is calculated separately for normal force (subscript n), shear force (subscript s) and pressure force (subscript p).

$$\rho_i \left[\frac{\partial \mathbf{v}_i}{\partial t} \right] = \rho_i \left[\frac{\partial \mathbf{v}_i}{\partial t} \right]_n + \rho_i \left[\frac{\partial \mathbf{v}_i}{\partial t} \right]_s + \rho_i \left[\frac{\partial \mathbf{v}_i}{\partial t} \right]_p \quad (7)$$

where $\mathbf{v}_i = \frac{\partial \mathbf{r}_i}{\partial t}$ is velocity of particle i , ρ is mass density. The term as to normal force (subscript n) and shear force (subscript s) can be calculated as follows,

$$\rho_i \left[\frac{\partial \mathbf{v}_i}{\partial t} \right]_n = \frac{d}{n_i^0} \sum_{j \neq i} \frac{2\sigma_{ij}^n}{\|\mathbf{r}_{ij}^0\|} w(\|\mathbf{r}_{ij}^0\|) = \frac{4d}{n_i^0} \sum_{j \neq i} \frac{(\mu_i + \mu_j)}{2} w(\|\mathbf{r}_{ij}^0\|) c_{ij}^n \frac{\mathbf{r}_{ij}}{\|\mathbf{r}_{ij}\|^2} \quad (8)$$

$$\rho_i \left[\frac{\partial \mathbf{v}_i}{\partial t} \right]_s = \frac{d}{n_i^0} \sum_{j \neq i} \frac{2\sigma_{ij}^s}{\|\mathbf{r}_{ij}^0\|} w(\|\mathbf{r}_{ij}^0\|) = \frac{4d}{n_i^0} \sum_{j \neq i} \mathbf{b}_{ij}^s, \quad \text{where, } \mathbf{b}_{ij}^s = \frac{(\mu_i + \mu_j)}{2} w(\|\mathbf{r}_{ij}^0\|) \frac{\mathbf{u}_{ij}^s}{\|\mathbf{r}_{ij}^0\|^2} \quad (9)$$

where d is a dimension parameter. In two dimensional space, the parameter d is 2. Weighting function w is introduced in order to model the interaction of neighboring particles. In MPS method, following equation is used as the weighting function.

$$w(|\mathbf{r}_{ij}^0|) = \begin{cases} \frac{r_e}{|\mathbf{r}_{ij}^0|} - 1 & (0 < |\mathbf{r}_{ij}^0| < r_e) \\ 0 & (r_e \leq |\mathbf{r}_{ij}^0|) \end{cases} \quad (10)$$

where r_e is influence radius which expresses the distance of particle interaction. n_i^0 is particle number density which can be calculated by the following equation.

$$n_i^0 = \sum_{i \neq j} w(|\mathbf{r}_{ij}^0|) \quad (11)$$

MPS method proposes use of constant value for particle number density n_i^0 in whole space. The pressure term is expressed by,

$$\rho_i \left[\frac{\partial \mathbf{v}_i}{\partial t} \right]_p = -\frac{d}{n_i^0} \sum_{j \neq i} \frac{2p_{ij}\mathbf{r}_{ij}^0}{|\mathbf{r}_{ij}^0||\mathbf{r}_{ij}^0|} w(|\mathbf{r}_{ij}^0|) \quad (12)$$

where $p_{ij} = \frac{p_i + p_j}{2}$, pressure at particle i , p_i is obtained by,

$$p_i = -\lambda_i (\epsilon_{rr})_i = -\lambda_i (div \mathbf{u})_i = -\lambda_i \frac{d}{n_i^0} \sum_{j \neq i} \frac{\mathbf{u}_{ij} \cdot \mathbf{r}_{ij}^0}{|\mathbf{r}_{ij}^0||\mathbf{r}_{ij}^0|} w(|\mathbf{r}_{ij}^0|) = -\lambda_i \frac{d}{n_i^0} \sum_{j \neq i} \frac{c_{ij}^n}{|\mathbf{r}_{ij}^0|} w(|\mathbf{r}_{ij}^0|) \quad (13)$$

where λ is Lame's constant.

2.1.3. Conservation of angular momentum

Angular momentum is not conserved in the discretization procedure in MPS because of equilibrium of finite small body, though original differential equation of motion conserves angular momentum. Therefore it is necessary to activate torque to cancel the torque caused by shear stress. Shear stress between particles i and j causes force \mathbf{F}_{ij} ,

$$\mathbf{F}_{ij} = m_i \left[\frac{\partial \mathbf{v}_{ij}}{\partial t} \right]_s = \frac{m_i 2d \sigma_{ij}^s}{\rho_i n_i^0 |\mathbf{r}_{ij}^0|} w(|\mathbf{r}_{ij}^0|) = \frac{4m_i d}{\rho_i n_i^0} \frac{\mu_i + \mu_j}{2} w(|\mathbf{r}_{ij}^0|) \frac{\mathbf{u}_{ij}^s}{|\mathbf{r}_{ij}^0|^2} = \frac{4m_i d}{\rho_i n_i^0} \mathbf{b}_{ij}^s \quad (14)$$

where, $m_i (= \rho_i D^2)$, D is diameter of particle i , the term $\partial \mathbf{v}_{ij} / \partial t$ is acceleration caused by shear stress between i and j . An equal and opposite force acts on particle i and j . Torque caused by the couple of force is expressed with outer product.

$$\mathbf{T}_{ij} = -\mathbf{r}_{ij} \times \mathbf{F}_{ij} \quad (15)$$

In order to cancel this torque, a half of the torque is given to particle i and j . This procedure is taken to every particle within influence distance of particle i .

$$I_i \left[\frac{\partial \omega_i}{\partial t} \right]_s = \sum_{j \neq i} \left[-\frac{1}{2} \mathbf{T}_{ij} \right] = 2d \sum_{j \neq i} \left(\frac{m_i}{\rho_i n_i^0} + \frac{m_j}{\rho_j n_j^0} \right) (\mathbf{r}_{ij} \times \mathbf{b}_{ij}^s) \quad (16)$$

where, $\omega_i (= \partial \theta_i / \partial t)$ is angular velocity, I_i is assumed to be $\rho_i D^4 / 6$ which is equal to rotary inertia of

square with length D on a side.

2.1.4 Verlet Method for time integration

Verlet method is adopted for integrating following equation of motion in this study.

$$\mathbf{M}\ddot{\mathbf{r}}_k + \mathbf{g}(\mathbf{r}_k, \dot{\mathbf{r}}_k) = \mathbf{f}_k \quad (17)$$

\mathbf{M} is diagonal mass matrix, \mathbf{g} is restoring force, which is function of position vector \mathbf{r}_k , velocity vector $\dot{\mathbf{r}}_k$. The acceleration vector is approximated by,

$$\ddot{\mathbf{r}}_k = \frac{\mathbf{r}_{k+1} - 2\mathbf{r}_k + \mathbf{r}_{k-1}}{\Delta t^2}, \quad \text{where, } \mathbf{r}_{k+1} = \mathbf{r}(t_k + \Delta t), \quad \mathbf{r}_k = \mathbf{r}(t_k), \quad \mathbf{r}_{k-1} = \mathbf{r}(t_k - \Delta t) \quad (18)$$

Substituting Eq.(18) into Eq.(17), we have,

$$\mathbf{M} \frac{\mathbf{r}_{k+1} - 2\mathbf{r}_k + \mathbf{r}_{k-1}}{\Delta t^2} + \mathbf{g}(\mathbf{r}_k, \dot{\mathbf{r}}_k) = \mathbf{f}_k \quad (19)$$

Arranging the equation, we have an equation to be solved.

$$\mathbf{r}_{k+1} = (2\mathbf{r}_k - \mathbf{r}_{k-1}) + \Delta t^2 \mathbf{M}^{-1} (\mathbf{f}_k - \mathbf{g}(\mathbf{r}_k, \dot{\mathbf{r}}_k)) \quad (20)$$

2.2. Viscous boundary and element wise Rayleigh damping

Many functions adopted in FEM can be also used in MPS because above mentioned formulation is derived mathematically from the governing equation. Viscous boundary condition is one of the functions widely used in FEM, which is important in earthquake response analysis. The following stress is given to viscous boundary in order to cancel reflection wave.

$$\tau(t) = \rho V \dot{r}(t) \quad (21)$$

where ρ is density, V is wave propagation velocity, $\dot{r}(t)$ is velocity of particle at the boundary. When upwardly propagating wave is specified as an input motion to a model (so-called 2E input), the following stress is given to the boundary.

$$\tau(t) = \rho V (2\dot{e}(t) - \dot{r}(t)) \quad (22)$$

where, $\dot{e}(t)$ is time history of input velocity. In MPS method with viscous boundary, the stress indicated in Eq.(22) is applied on particles at viscous boundary in addition to external force f and restoration force g .

$$m\ddot{r}_k^b = f_k - g(\dot{\mathbf{u}}_k, \mathbf{u}_k) + D\rho V (2\dot{e}_k - \dot{r}_k^b) \quad (23)$$

where m is mass of a particle which is assumed to be $\rho_i D^2$, D is a particle diameter. We have following formulation to estimate acceleration of a particle at viscous boundary.

$$\ddot{r}_k^b = \frac{1}{D^2 \rho} (f_k - g(\dot{\mathbf{u}}_k, \mathbf{u}_k)) + \frac{V}{D} (2\dot{e}_k - \dot{r}_k^b) \quad (24)$$

In earthquake response analysis with finite element method, element-wise Rayleigh damping is often used.

$$\mathbf{M}\ddot{\mathbf{r}}_k + \mathbf{C}_M\dot{\mathbf{r}}_k + \mathbf{C}_K\dot{\mathbf{u}}_k + \mathbf{g}(\mathbf{u}_k) = \mathbf{f}_k \quad (25)$$

where k indicate time step, \mathbf{g} is restoration force depending on deformation \mathbf{u}_k , which is deformation that rigid rotation component is removed. \mathbf{M}, \mathbf{f}_k are mass matrix and external force vector. The damping term is divided into two parts, \mathbf{C}_M related to the mass and \mathbf{C}_K related to the stiffness. Damping ratio h_i is allocated to each particle i .

$$\mathbf{C}_M = a_1 \mathbf{H} \mathbf{M}, \quad \mathbf{C}_K = a_2 \mathbf{H} \frac{d\mathbf{g}}{d\mathbf{u}} \quad \text{where, } \mathbf{H} = \begin{bmatrix} h_1 & & & \mathbf{0} \\ & h_2 & & \\ & & \ddots & \\ \mathbf{0} & & & h_n \end{bmatrix} \quad (26)$$

\mathbf{H} is a diagonal matrix which stores the damping ratio of each particle, h_i . Particle methods generally do not have stiffness matrix unlike FEM. Instead Matrix $d\mathbf{g}/d\mathbf{u}$ is used in the proposed formulation. Substituting Eq.(26) to (25), we have

$$\ddot{\mathbf{r}}_k + a_1 \mathbf{H} \dot{\mathbf{r}}_k + a_2 \mathbf{H} \mathbf{M}^{-1} \frac{d\mathbf{g}}{d\mathbf{u}} \dot{\mathbf{u}}_k + \mathbf{M}^{-1} \mathbf{g}(\mathbf{u}_k) = \mathbf{M}^{-1} \mathbf{f}_k \quad (27)$$

First order Tailor's expansion gives the equation,

$$\mathbf{g}(\mathbf{u}(t - \Delta t)) = \mathbf{g}(\mathbf{u}(t)) - \Delta t \frac{d\mathbf{g}}{d\mathbf{u}} \frac{d\mathbf{u}}{dt} \quad (28)$$

By deforming the equation, we have,

$$\frac{d\mathbf{g}}{d\mathbf{u}} \dot{\mathbf{u}}_k = \frac{\mathbf{g}(\mathbf{u}_k) - \mathbf{g}(\mathbf{u}_{k-1})}{\Delta t} \quad (29)$$

It is noted that time t and $t - \Delta t$ are denoted by using subscript $k, k-1$. Substituting Eq.(29) into Eq.(27), we have

$$\ddot{\mathbf{r}}_k = \mathbf{M}^{-1} \mathbf{f}_k - a_1 \mathbf{H} \dot{\mathbf{r}}_k - \left(\frac{a_2}{\Delta t} \mathbf{H} + \mathbf{I} \right) \mathbf{M}^{-1} \mathbf{g}(\mathbf{u}_k) + \frac{a_2}{\Delta t} \mathbf{H} \mathbf{M}^{-1} \mathbf{g}(\mathbf{u}_{k-1}) \quad (30)$$

where \mathbf{I} is unit matrix. Please refer to Yoshida et al (2010) for detail.

2.3. Formulation for failure phenomenon

Failure behavior is modeled by simple operation as to maximum shear stress and disconnection of particles like DEM. Mohr-Coulomb criteria gives maximum shear stress τ_{\max} .

$$\tau_{\max} = c_{ij} + \sigma_{ij}^n \tan \phi_{ij} \quad (31)$$

where, σ_{ij}^n is normal stress between particle i and j , c_{ij} is cohesion, ϕ_{ij} is internal friction angle. They express mean value of particles i and j . When σ_{ij}^n is negative (tensile stress), maximum shear stress is c_{ij} . It is noted that these parameters are given to each particle, and these parameters do not indicate macro (total) strength obtained by compression test of soil. DEM has the same problem that parameters given to each particle does not mean macro strength. Therefore calibration analysis is necessary to determine input (micro) strength parameter to realize specific macro strength.

Inter-particle stress σ_{ij}^n can be estimated by the following equation.

$$\sigma_{ij}^n = 2\mu_{ij} \frac{\mathbf{u}_{ij} \cdot \mathbf{r}_{ij}}{|\mathbf{r}_{ij}| |\mathbf{r}_{ij}^0|} + p_{ij} = 2\mu_{ij} \frac{c_{ij}^n}{|\mathbf{r}_{ij}^0|} + p_{ij} \quad (32)$$

where, μ_{ij} is Lame's constant, p_{ij} can be obtained by Eq.(13). Shear stress is,

$$\tau_{ij}^s = 2\mu_{ij} \frac{\mathbf{u}_{ij}^s}{|\mathbf{r}_{ij}^0|}, \quad \text{where, } \mathbf{u}_{ij}^s = \mathbf{u}_{ij} - \mathbf{u}_{ij}^n, \quad \mathbf{u}_{ij}^n = \frac{(\mathbf{u}_{ij} \cdot \mathbf{r}_{ij}) \mathbf{r}_{ij}}{|\mathbf{r}_{ij}| |\mathbf{r}_{ij}|} \quad (33)$$

When $\tau_{\max} \leq |\tau_{ij}^s|$, rotation angles θ_i^{ij} , θ_j^{ij} and initial vector \mathbf{r}_{ij}^0 corresponding to particles i, j are updated as follows such that the condition $|\tau_{ij}^s| = \tau_{\max}$ is satisfied.

$$\mathbf{r}_{ij}^0 = \mathbf{r}_{ij}^0 - \frac{\tau_{\max}}{|\tau_{ij}^s|} \mathbf{u}_{ij}^s \quad (34)$$

$$\theta_i^{ij} = \theta_i - \tan^{-1}\left(\frac{\tau_{\max}}{\mu_{ij}}\right), \quad \theta_j^{ij} = \theta_j - \tan^{-1}\left(\frac{\tau_{\max}}{\mu_{ij}}\right) \quad (35)$$

The rotation angles θ_i^{ij} , θ_j^{ij} are used in matrix \mathbf{R} in Eq.(2) which removes rigid rotation component.

$$\mathbf{R}_i = \begin{bmatrix} \cos(\theta_i - \theta_i^{ij}) & -\sin(\theta_i - \theta_i^{ij}) \\ \sin(\theta_i - \theta_i^{ij}) & \cos(\theta_i - \theta_i^{ij}) \end{bmatrix}, \quad \mathbf{R}_j = \begin{bmatrix} \cos(\theta_j - \theta_j^{ij}) & -\sin(\theta_j - \theta_j^{ij}) \\ \sin(\theta_j - \theta_j^{ij}) & \cos(\theta_j - \theta_j^{ij}) \end{bmatrix} \quad (36)$$

The above mentioned operation with respect to shear stress does not disconnect interaction between particles. Normal stress is used for the judgment of disconnection of particles. When inter-particle normal stress σ_{ij}^n is less than tensile strength c_t , the particles are disconnected. It is noted that tensile stress is negative.

$$\sigma_{ij}^n < c_t \quad (37)$$

We assume that tensile strength is equal to cohesion, namely, $c_t = -c_{ij}$ in the following numerical examples.

Disconnection or large deformation causes new contact of a pair of particle. When particles i and j are judged to be newly contacted by distance between them, the position vector \mathbf{r}_{ij}^0 and angle θ_i^{ij} , θ_j^{ij} at the moment are memorized. The reaction forces due to Lame's constant μ_{ij} , which are calculated by Eq.(8) and (9), are considered. This operation for new contacted particles is perfectly same as that of DEM. Please refer to Yoshida (2011) for detail.

3. TWO DIMENSIONAL WAVE PROPAGATION

The validity of proposed viscous boundary and particle-wise Rayleigh damping is examined by the comparison with wave propagation calculated by FEM. The model properties are summarized in Table.1. Fig. 1 shows a slope model for the FEM analysis. The height of the slope is 161 m. There are three layers with distinct properties including damping ratio. The model for MPS method is also constructed with 77,181 particles of radius 1.0 m.

The bottom of the model is viscous boundary, while side boundaries are free in horizontal and vertical direction. Ricker wavelet with central frequency 4 Hz, which is shown in Fig. 2, is input to the viscous boundary in both vertical and horizontal direction at the same time. Fig. 3 shows the comparison of

response acceleration time history at the slope top. The agreement is very good though the response includes many factors like coupling from S-wave to P-wave or from S-wave to P-wave, reflection at layer boundaries, Rayleigh damping and viscous boundary. It can be concluded that MPS method is good enough to simulate the dynamic response of slope.

Table 1. Soil properties of model for the wave propagation

Property	Unit	Soft ground	Ground	Rock
Unit Weight	kN/m ³	20	25	26
Shear Modulus	MPa	720	4200	11000
Poisson's Ratio	—	0.40	0.37	0.35
Damping Ratio	%	7.0	3.0	3.0

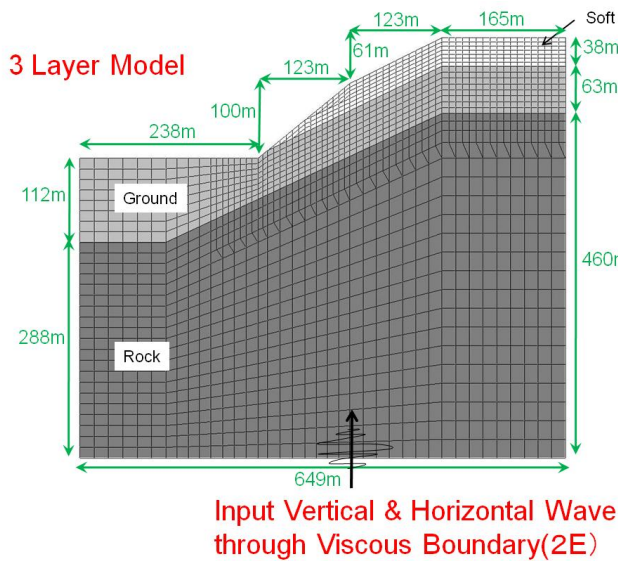


Figure 1. A slope model for FEM

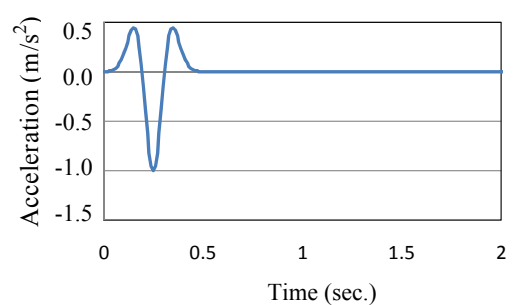


Figure 2. Input motion (acceleration)

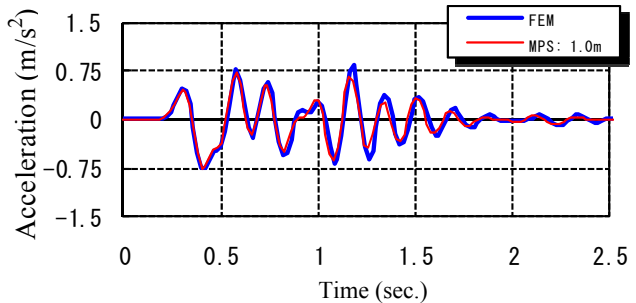


Figure 3. Comparison of response at slope top by MPS method and FEM

4. SIMULATION OF EXPERIMENT OF SLOPE FAILURE

Simulation of slope failure centrifugal test is performed by MPS method. The test was carried out in order to study the behaviour of slope failure. Outline of the simulation result is here introduced just briefly. A sinusoidal motion in Fig. 4 is used as an excitation input to the shaking table after static 50g force is applied to vertical direction. The maximum amplitude of the excitation motion (maximum acceleration) is increased step by step. The slope model collapsed when maximum acceleration of input motion is 600gal. The slope model is shown in Fig. 5. The height of slope is 50 cm in 50g, which can be interpreted to be 25 m in 1g.

Fig. 5 also illustrates the failure shape obtained by the experiment and the simulation by MPS method. The simulation result shows very good agreement with experiment. Many simulations are, however, performed to find strength parameters which can reproduce the experimental result. Fig. 5 shows the best case in the many try-and-error cases.

5. CONCLUSION

The basic formulation of MPS method is described. Particle-wise Rayleigh damping and viscous boundary for MPS method are proposed for earthquake response analysis. MPS method can be interpreted as extended DEM (Discrete Element Method), which is derived mathematically from wave equation. Validity of the proposed damping ratio and viscous boundary is demonstrated through two dimensional wave propagation simulation. Collapse simulation is also shown to demonstrate the applicability of MPS method to highly nonlinear failure phenomenon briefly.

As future topics, quantitative study with collapse experiment is required to confirm the usefulness of MPS method. The determination of input strength parameters based on ordinary soil test results is also one of important issues in MPS method as same as in DEM.

REFERENCES

- Chikazawa, Y., Koshizuka, S. and Oka, Y. 2001. A Particle Method for Elastic and Visco-plastic Structures and Fluid-structure Interactions, Computational Mechanics, 27, pp. 97-106
 Koshizuka, S., Tamako, H. and Oka, Y. 1995. A Particle Method for Incompressible Viscous Flow with Fluid Fragmentation, Comput. Fluid Dynamics J., 4, pp. 29-46
 Koshizuka, S. and Oka, Y. 1996. Moving-Particle Semi-implicit Method for Fragmentation of Incompressible Fluid, Nucl. Sci. Eng., 123, pp. 421-434
 Yoshida, I. and Ishimaru, M. 2010. Basic Study on Earthquake Response Analysis with Using MPS Method, J. of JSCE, A, Vol.66, No.2, pp.206-218 (in Japanese)
 Yoshida, I. 2011. Basic study on failure analysis with using MPS method, Journal of Japan Society of Civil Engineers, A2, Vol.67, No.1, pp.93-104, 2011.8 (in Japanese)

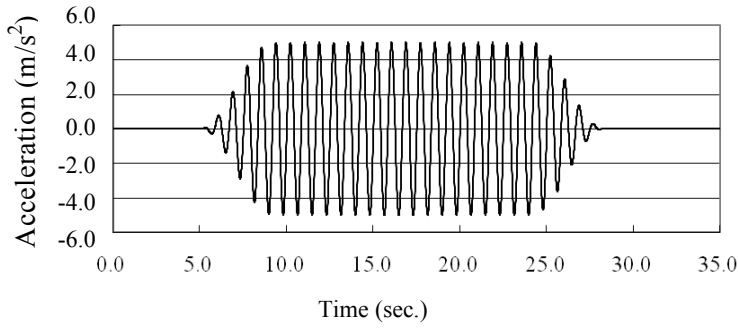


Figure 4. Time history of input sinusoidal wave

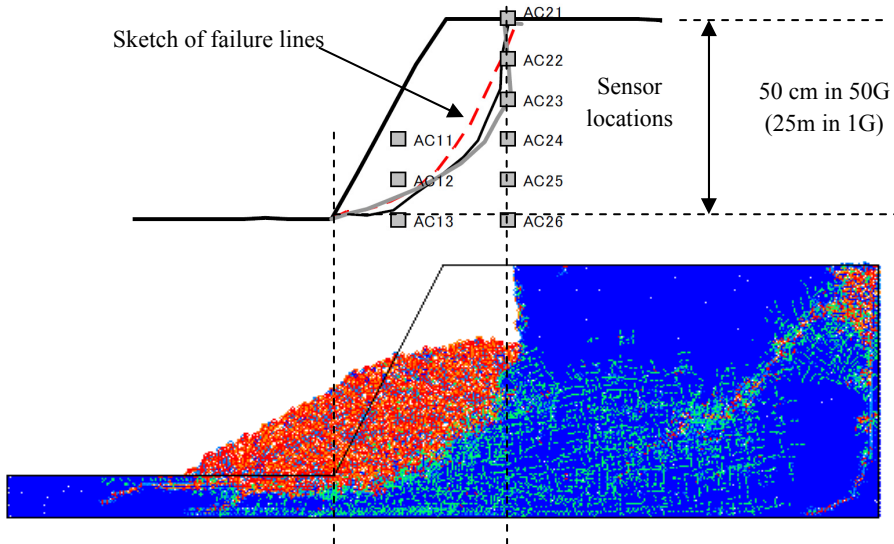


Figure 5. Collapse line obtained by experiment and numerical simulation by MPS method